Pliocene to Recent shallow-water contourite deposits on the shelf and shelf edge off south-western Mallorca, Spain

Thomas Philippe Vandorpe, David Van Rooij, Dorrik A. V. Stow & Jean-Pierre Henriet

Geo-Marine Letters
An International Journal of Marine Geology

ISSN 0276-0460
Volume 31
Combined 5-6

Geo-Mar Lett (2011) 31:391-403
DOI 10.1007/s00367-011-0248-9

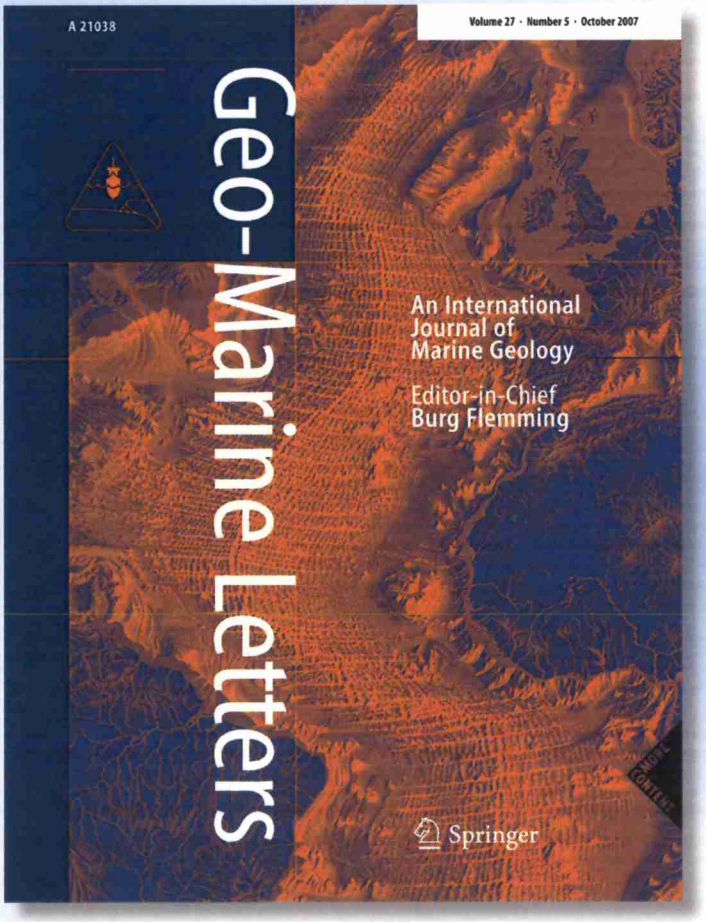

Springer

Geo-Mar Lett (2011) 31:391–403
DOI 10.1007/s00367-011-0248-9

ORIGINAL

Pliocene to Recent shallow-water contourite deposits on the shelf and shelf edge off south-western Mallorca, Spain

Thomas Philippe Vandorpe · David Van Rooij · Dorrik A. V. Stow · Jean-Pierre Henriet

Received: 22 October 2010 / Accepted: 16 June 2011 / Published online: 24 June 2011

Abstract This paper presents evidence for the presence of shallow-water contourite drifts on the south-western shelf and shelf edge off Mallorca in water depths between 150 and 275 m. These are called the Mallorca contourite depositional system (CDS). The elongate-mounded shallow-water CDS in this area is ascribed to an offshoot of the Balearic Current, which flows north to south through the Mallorca Channel as part of the overall thermohaline circulation in the Mediterranean Sea. Drift geometry suggests that the north–south current is deflected into an east–west flow pattern by interaction with a marked seafloor bathymetry, associated with major fault displacement. Four seismic units separated by three prominent discontinuities can be identified. The three internal discontinuities are correlated to large-scale basin-wide events: the lower Pliocene revolution (4.2 Ma), the upper Pliocene revolution (2.4 Ma) and the mid-Pleistocene revolution (0.9 Ma). The Plio-Quaternary succession has been deposited on top of a Miocene reef, which serves as an acoustic basement and is affected by a large fault, offsetting the basement on average by 150 m. Marked erosional features throughout and further incision of the Sant Jordi Channel along the basement fault in the Pleistocene deposits indicate stronger currents in this period. The Pleistocene deposits also show a pronounced cyclicity, which is tentatively ascribed to climatic variations and the effects of eustatic sea-level fluctuation over the south-western Mallorca shelf at that time.

Responsible guest editor: E. Llave

T. P. Vandorpe (✉) · D. Van Rooij · J.-P. Henriet
Renard Centre of Marine Geology, Department of Geology & Soil Science, Ghent University,
Krijgslaan 281 S8,
9000 Ghent, Belgium
e-mail: thomas.vandorpe@ugent.be

D. A. V. Stow
Institute of Petroleum Engineering, Heriot-Watt University,
Edinburgh EH14 4AS, UK

Introduction

The term *contourites* originally referred to deep-sea deposits under the influence of thermohaline circulation (Heezen et al. 1966) but, as ever more contourite systems were discovered in progressively shallower water settings, its definition has been adapted. Faugères and Stow (1993) broadened the definition to include deposits in water depths below 500 m formed by a deep and steady geostrophic current. Later, Viana et al. (1998) subdivided contourites into three categories, based on their morphological setting and water depth: deep-water (>2,000 m), mid-water (2,000–300 m) and shallow-water (200–50 m) contourites. Stow et al. (2002) proposed using "shallow-water contourites" for those systems above 300 m water depth and Viana et al. (2007) applied this term to deposits in shallow-water settings where the influence of geostrophic currents outweighs that of storm- and wind-induced currents.

Examples of shallow-water contourites are still rather scarce, especially compared to mid- and deep-water systems. They result from the action of relatively intense bottom-hugging currents and may be aided in their formation by storm-induced currents (Viana et al. 1998). In the Mediterranean, shallow-water contourites are known from (amongst others) the southern Adriatic Sea and Gela Basin, Sicily Strait (Verdicchio and Trincardi 2008a) and from the Moroccan margin (Ercilla et al. 2002). In the present study, a newly discovered shallow-water contourite

depositional system is reported from the south-western Mallorca shelf (Fig. 1).

Little is known about the sedimentological and oceanographic evolution of the south-western Mallorca shelf (see Just et al. 2011 for recent overview). Interpretation of a sparker seismic profile located close to the shelf edge in this area indicates the presence of a Miocene reef overlain by Plio-Quaternary sedimentary deposits and a steep fault, offsetting the reef by about 175 m (Stanley et al. 1976). The sedimentary succession on top of the reef consists of biogenic sands and gravels (carbonate content of 77–84%; Acosta et al. 2002; Betzler et al. 2011).

In 2003, the Vrije Universiteit Amsterdam and the Renard Centre of Marine Geology (Ghent University) conducted a joint survey on the south-western Mallorca shelf and shelf edge. The resulting grid of high-resolution seismic profiles, covering an area of about 250 km^2 (Fig. 1), has been used here to (1) derive a local

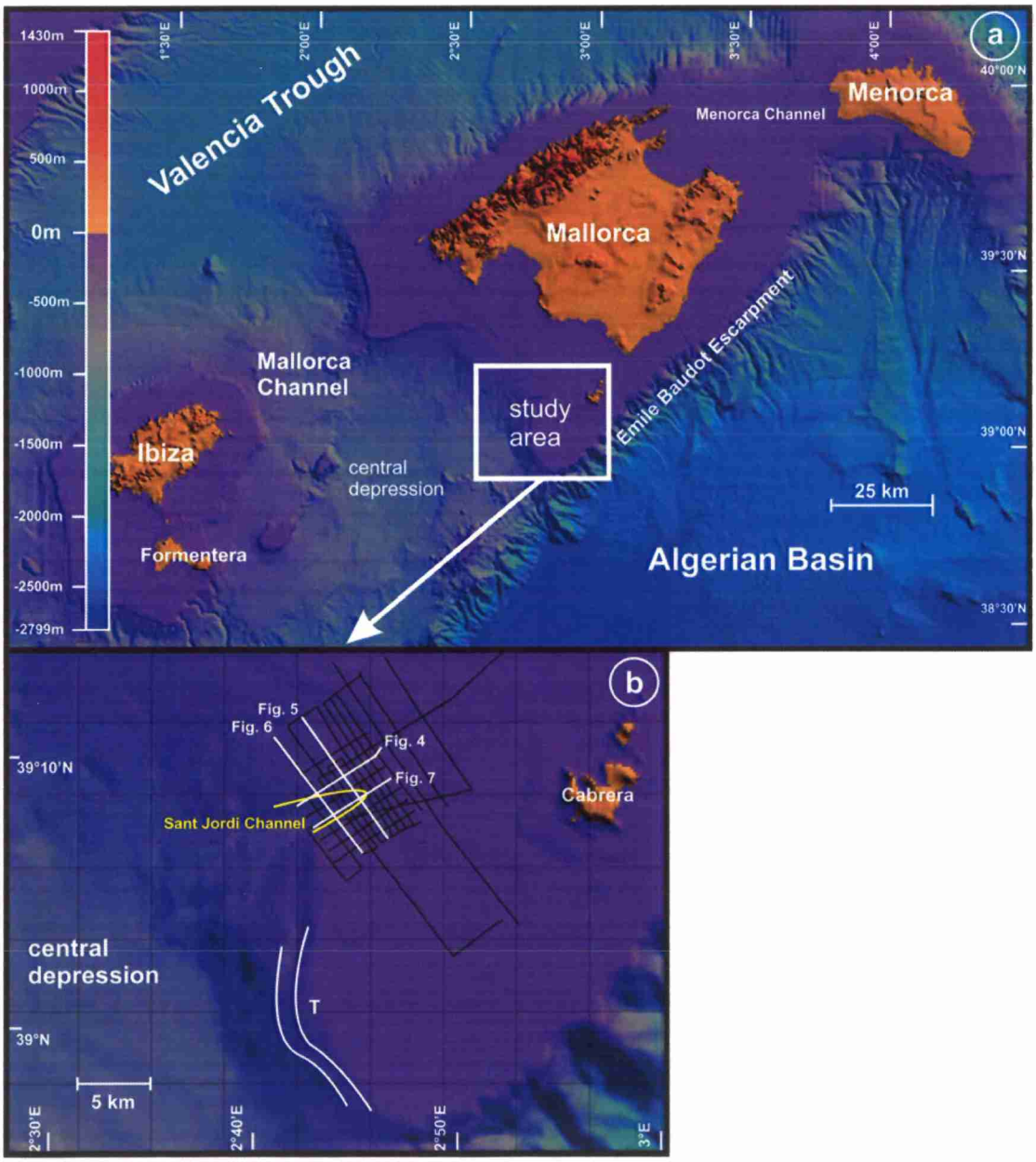

Fig. 1 **a** Locations of the Balearic Promontory, bounded by the Valencia Trough in the north and the Algerian Basin in the south, and of the study area on the south-western shelf and shelf edge southwest of Mallorca. **b** Multibeam bathymetric map of the study area (extracted from Acosta et al. 2004), showing the seismic grid. The two terraces (*T*) along the shelf edge to the south disappear upon reaching the mouth of the Sant Jordi Channel (*yellow line*)

stratigraphic framework, (2) determine the influence of the local oceanographic setting on sedimentation and (3) infer the evolution of the contouritic processes in tentative correlation with local oceanographic processes.

Physical setting

Geological setting

The study area is a part of the Balearic Promontory, which is a structural elevation consisting of the three main Balearic islands (from west to east): Ibiza, Mallorca and Menorca (Fig. 1). Mallorca is the biggest island and has the most extensive shelf, connected to the Menorca shelf and with water depths ranging from 150 ms TWT (two-way travel time) in the northeast to 275 ms in the southwest. The shelf southwest of Mallorca can be subdivided into two main regions. The northern region (about 20 km wide) has a less pronounced shelf break and a gentle slope (about 0.5°) towards a central depression, whereas the southern region (25 km wide) displays a more pronounced shelf edge and a steeper slope with at least two terraces (Fig. 1). At the intersection of the two regions there is a prominent channel (some 5 km long) which has a straight southern and a curved northern margin (Fig. 1). This channel is here named the *Sant Jordi Channel*, after the nearby town of Colònia Sant Jordi on Mallorca.

The present-day physiography of the south-western Mallorca shelf is the result of structural displacements from the Late Miocene to recent times, along two main structural directions: NE–SW and NW–SE (Stanley et al. 1976). In general, the region underwent relatively rapid subsidence during the Pliocene and more gentle subsidence during the Pleistocene (Stanley et al. 1976). The Mallorca Channel, with a maximum depth exceeding 1,000 m and a thick fill of Pliocene to Recent sediments, is considered to have resulted from this continued subsidence. During the Messinian, the Mallorca shelf was wholly exposed and subject to subaerial (fluvial) erosion (e.g. Just et al. 2011), while during the Pleistocene eustatic sea-level oscillations there was an alternation between subaerial/submarine exposure and marine transgression (Acosta et al. 2001).

Oceanographic setting

Over the Balearic Promontory, there is an exchange between two different water masses (Fig. 2): cooler and more saline waters from the north (Winter Intermediate Water), which originate in the Gulf of Lyons, and warmer waters from the south originating from modified Atlantic waters (Pinot et al. 2002). The Mallorca Channel presently has two currents passing through it (Fig. 2): a north–south-oriented offshoot of the Balearic Current (cooler and more saline waters) at the bottom and a south-north-oriented offshoot of an anticylonic gyre of inflowing Atlantic water on the top (Pinot et al. 2002; Monserrat et al. 2008; Bardají et al. 2009). The strength of the Balearic Current offshoot is determined by that of eddies (consisting of Winter Intermediate Water) prevailing in the Gulf of Valencia, in turn controlled by the severity of the preceding winter (Pinot et al. 2002; Monserrat et al. 2008). A study carried out by Werner et al. (1993) indicates that storm-induced currents in the area can reach speeds in the order of 50 cm/s and flow from northwest to southeast. As the effect of wind stress can extend up to a few hundred of meters through the water column via friction of different water layers (Pickard and Emery 1990), these storms may have a direct effect on seafloor deposition in the study area.

Materials and methods

During the high-resolution seismic survey carried out in the south-western part of the Mallorca shelf and shelf edge in 2003 (Fig. 1), 46 lines were acquired using a SIG sparker (0.3–0.5 kJ energy pulses with an average frequency of 700 Hz) and a single-channel streamer. Most of the lines are approx. 15 km long and have either a NW–SE or NE–SW orientation. The penetration of the profiles is about 700 ms TWT. The seismic data were processed applying swell and multiple removal, a bandpass filter (0–1,350 Hz), and migration at a constant velocity of 1,500 m/s.

The multibeam bathymetric data, initially described and reported by Acosta et al. (2004), were obtained using Simrad EM-12S and EM-1000 systems during several cruises conducted from 1974 to 1998 as part of the Spanish Exclusive Economic Zone Program. They cover the entire Balearic region (Fig. 1)—about 60,000 km^2—and have an accuracy of approx. 10 m.

Results

Acoustic basement

An acoustic basement can be observed in all the seismic profiles examined, at about 20 to 250 ms TWT below seafloor (Fig. 3). This basement is characterized by high acoustic reflectivity with only a few short and discontinuous reflectors below (Figs. 4, 5 and 6). Broadly, there are two distinct subdivisions of the study area: a south-eastern

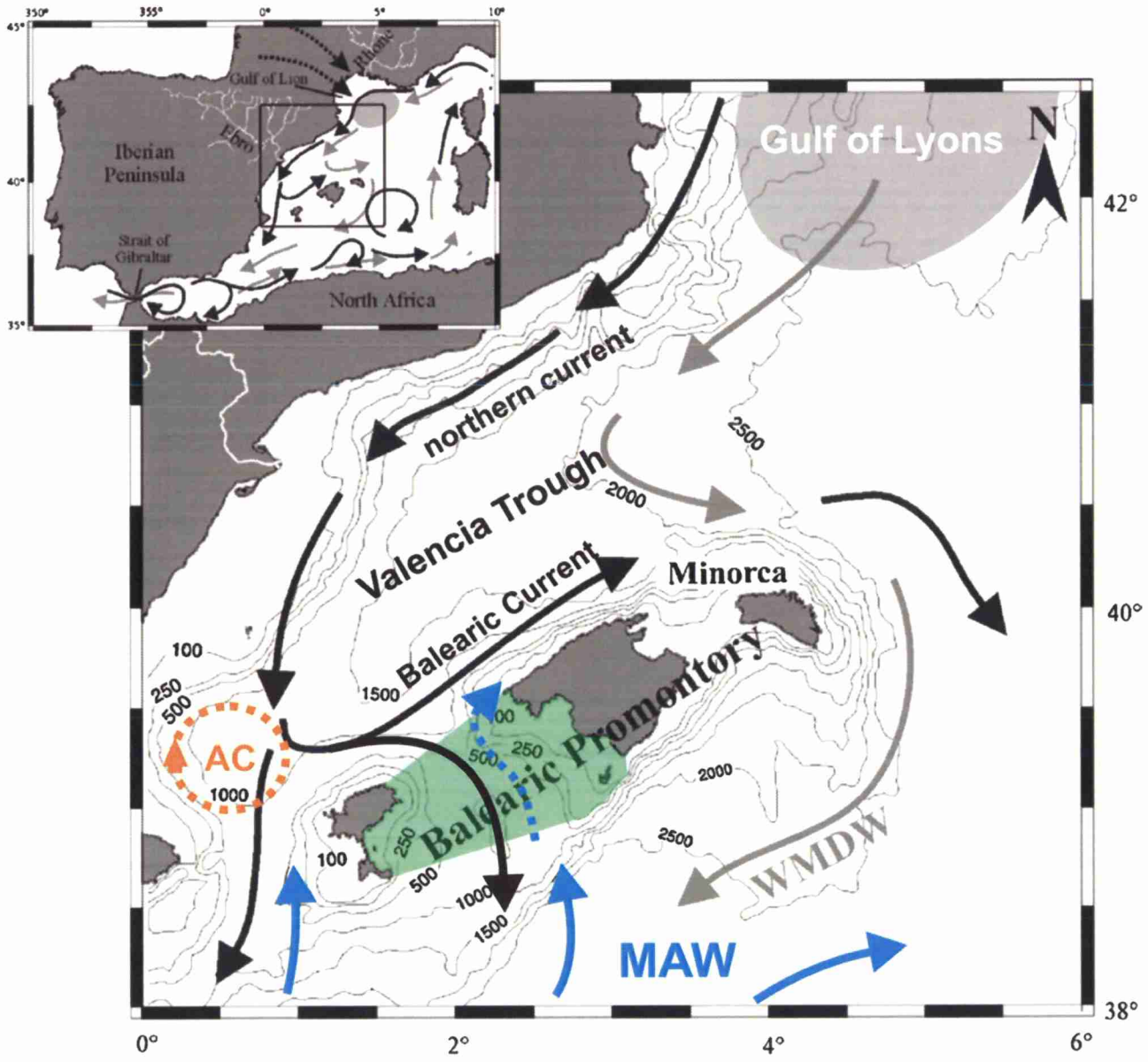

Fig. 2 Oceanographic setting of the Balearic Promontory (adapted from Frigola et al. 2008). The so-called northern current originates in the Gulf of Lyons and either flows through the Ibiza Channel or gets diverted into the Balearic Current. An offshoot of the Balearic Current flows through the Mallorca Channel (*black arrow in green-shaded channel*), consisting of Winter Intermediate Water and surface waters. Western Mediterranean Deep Water (*WMDW*) originates (partly) in the Gulf of Lyons, and flows east and south of the promontory towards the Strait of Gibraltar (*grey arrows*). Modified Atlantic waters (*MAW*) originate from Atlantic waters inflowing through the Strait of Gibraltar, and continuing through the Ibiza and Mallorca channels (*blue arrows*). *AC* Anticyclonic gyre

sector, with a relatively shallow depth to the basement (on average 150 ms below sea surface) and a sedimentary cover of about 25 ms TWT, and a north-western sector where the basement is situated about 450 ms below the sea surface covered by up to 250 ms of sediments (Fig. 3). The boundary between these two sectors is defined by a steep and prominent fault, which offsets the basement by 200–250 ms TWT.

Sedimentary units

Four seismic units were recognized based on the presence of discontinuities and seismic facies variability. Unit 1 lies directly on top of the basement, R, while its upper boundary is formed by discontinuity D1 (Figs. 5 and 6). Unit 2 lies on top of D1 in the west and directly on top of the basement, R, in the east (Fig. 5). This unit is capped by

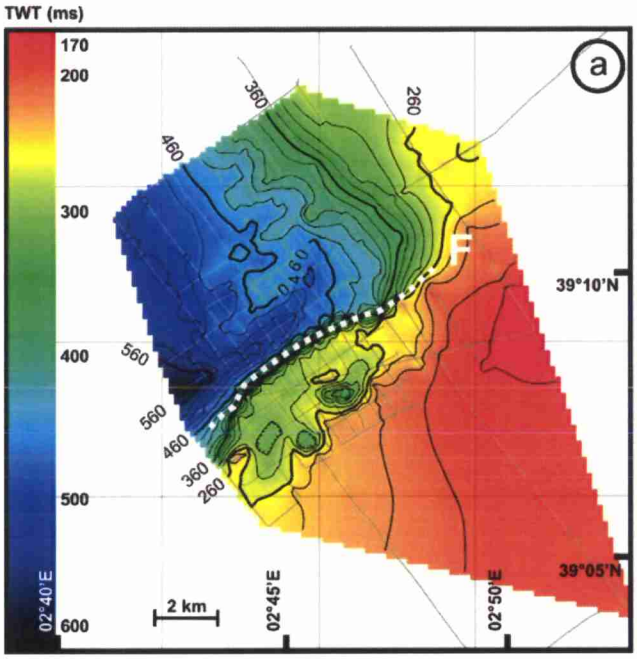

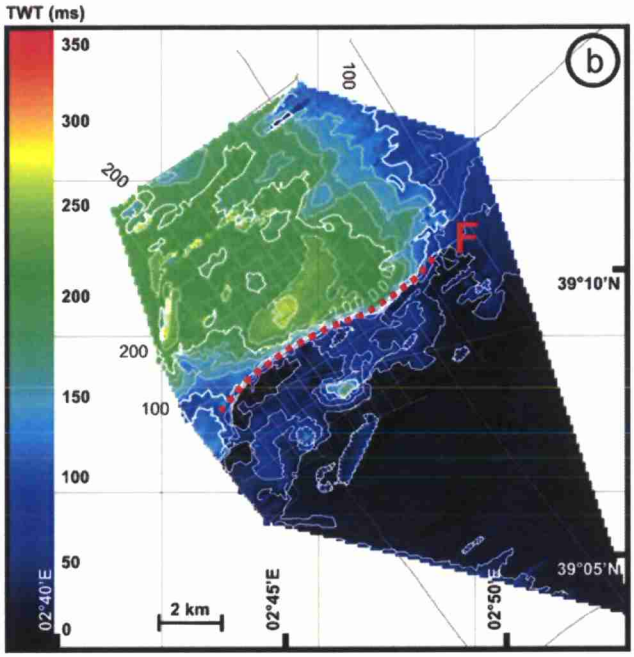

Fig. 3 **a** Isopachyte map showing the depth (in ms TWT) to the acoustic basement, with evidence of a large fault (*F*, *dashed line*) demarcating the boundary between a northern and southern sector. **b** Isopachyte map showing the thickness (in ms TWT) of the sedimentary cover, with evidence of the steep basement fault (*dashed line)*

an erosional discontinuity, D2. Unit 3 overlies D2 and is capped by discontinuity D3. The uppermost unit is deposited on top of D3 and has the seafloor as its upper boundary.

Unit 1

Unit 1, bounded by the basement and D1, is present only in the west–southwest part of the seismic grid. The thickest deposits (up to 100 ms TWT) of this unit are found immediately northwest of the basement fault and gradually diminish eastwards and northwards (Fig. 4). The internal configuration of the unit is characterized by wavy to hummocky, parallel to sub-parallel strata and locally by a more chaotic facies (Figs. 4 and 6). Unit 1 deposits generally drape over the irregular basement surface. Faults dipping to the northwest are observed throughout, while close to the basement fault there are many small vertical faults displaying offsets in the order of 1–2 ms TWT (Fig. 6).

Unit 2

Unit 2 is deposited in between discontinuities D1 and D2 in the western part of the seismic grid, except for a small sector northwest of the basement fault where the unit is topped by D3 (Fig. 5). In the east, the unit is deposited between the basement and D2 (Fig. 5). Unit 2 has its thickest deposits in the northeast. Generally, an increase in thickness occurs from the southwest (±50 ms TWT) to the northeast (>100 ms).

Unit 2 is the acoustically most transparent unit of the sedimentary succession and shows two different seismic facies. Facies 1 displays semi-parallel, wavy and continuous reflectors, locally interrupted by cut-and-fill structures (on average 25 ms TWT thick). These incisions display southeast-dipping, onlapping infill and are observed 1.5 to 4 km to the northwest of the basement fault (Figs. 5 and 6). The profile in Fig. 4 shows seven of these cut-and-fill structures. In some profiles (e.g. Fig. 5), moats (at most 20 ms TWT deep) can be distinguished close to the basement fault. Facies 2 has a chaotic configuration with lenticular, discontinuous and hummocky strata (Fig. 5).

In profiles across the steep basement fault, facies 1 is generally encountered immediately to the southeast. Facies 2 occurs about 2–3 km to the northwest of facies 1, with a gradual transition between the two. In some areas, especially close to the basement fault, there are numerous small vertical faults with offsets in the order of 1–2 ms TWT, similar to those in unit 1.

Unit 3

This unit is deposited on top of the erosional discontinuity D2, which shows incisions up to 150 ms TWT, and is overlain by discontinuity D3. Unit 3 fills several of these

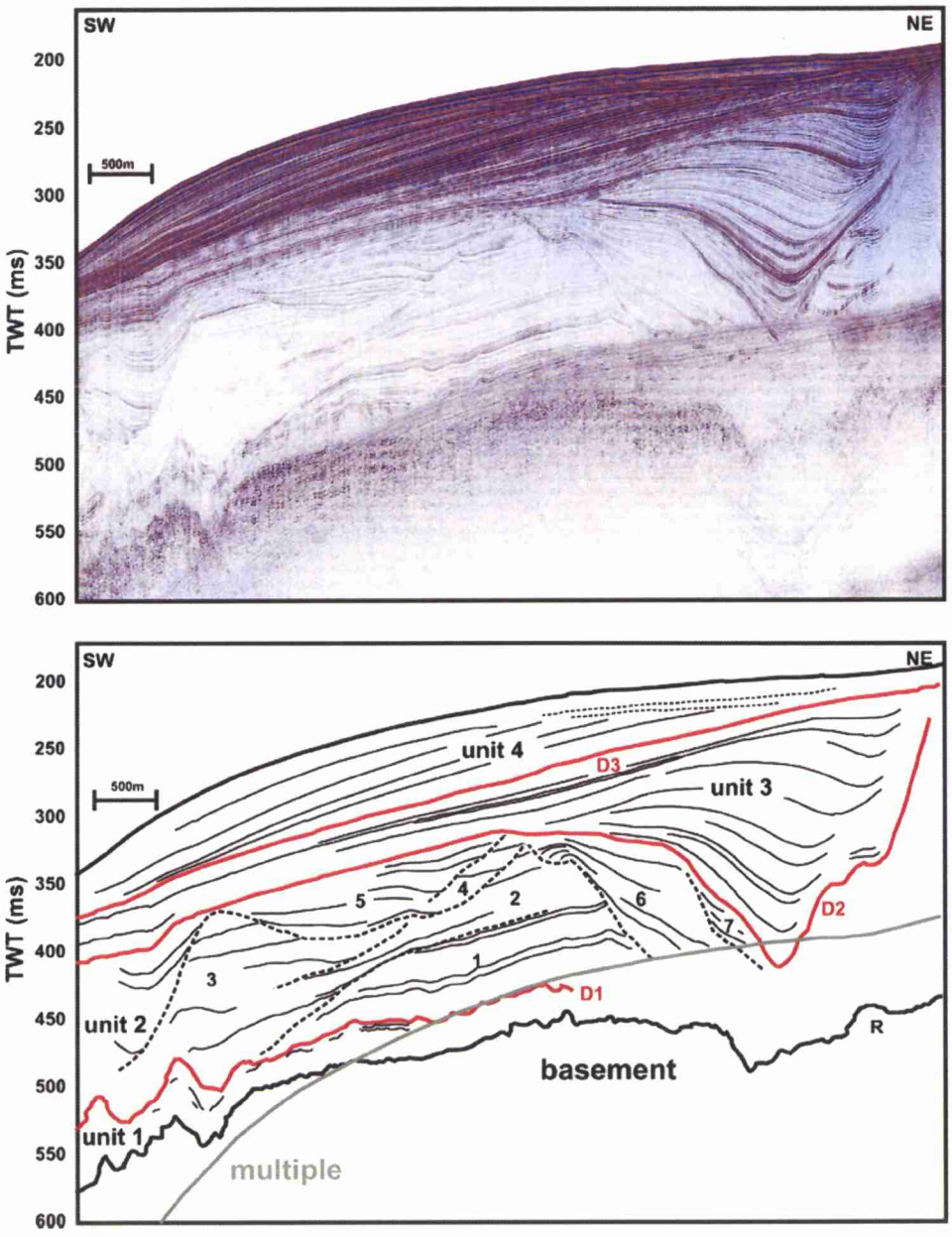

Fig. 4 Profile parallel to and immediately north of the basement fault, showing the acoustic basement, four depositional units and three discontinuities (for profile location, see Fig. 1b). Facies 1 is present in unit 2. Discontinuity D2 cuts deeply into unit 2, creating a channel filled by onlapping deposits of unit 3. Unit 3 (except for the channel infill) and unit 4 show parallel reflectors. A thin layer of surface sediment covers the top of unit 4 (*dashed lines*). Numbers *1* to *7* denote the subunits of unit 2

erosional features, including (1) a large incision in the eastern part of the seismic grid with depths of approx. 150 ms TWT (Fig. 4), (2) an amphitheatre-shaped depression in the west (about 140 ms deep), (3) a large channel (on average 50 ms deep) parallel to the basement fault (Fig. 6)—although in some places the channel is infilled with seismic unit 4 (e.g. Fig. 5)—and (4) small 20–30 ms deep irregular incisions in the north of the study area (Figs. 5 and 6). The thickness of this unit typically ranges between 20 and 75 ms TWT, whereas within these erosional features it is up to 150 ms.

Unit 3 displays a marked increase in amplitude compared to the underlying unit 2. This unit fills the aforementioned erosional features and drapes the older deposits outside of these. The sedimentary drape is composed of six subunits distinguished by alternating reflector packages having high and low amplitudes (Figs. 4, 5 and 6). The subunits have a sigmoidal geometry in the Sant Jordi Channel along the basement fault (Fig. 7). In the infill section, dipping and onlapping reflectors are observed which level out towards the sedimentary drape. The onlap always occurs on the south-western or south-eastern margin of the incision (Figs. 4, 5 and 6). In several NW–SE-oriented profiles, two channels can be seen to have been cut into the sedimentary drape of this unit. The internal reflectors of the deposits display onlap terminations towards the south-eastern edges (Fig. 6).

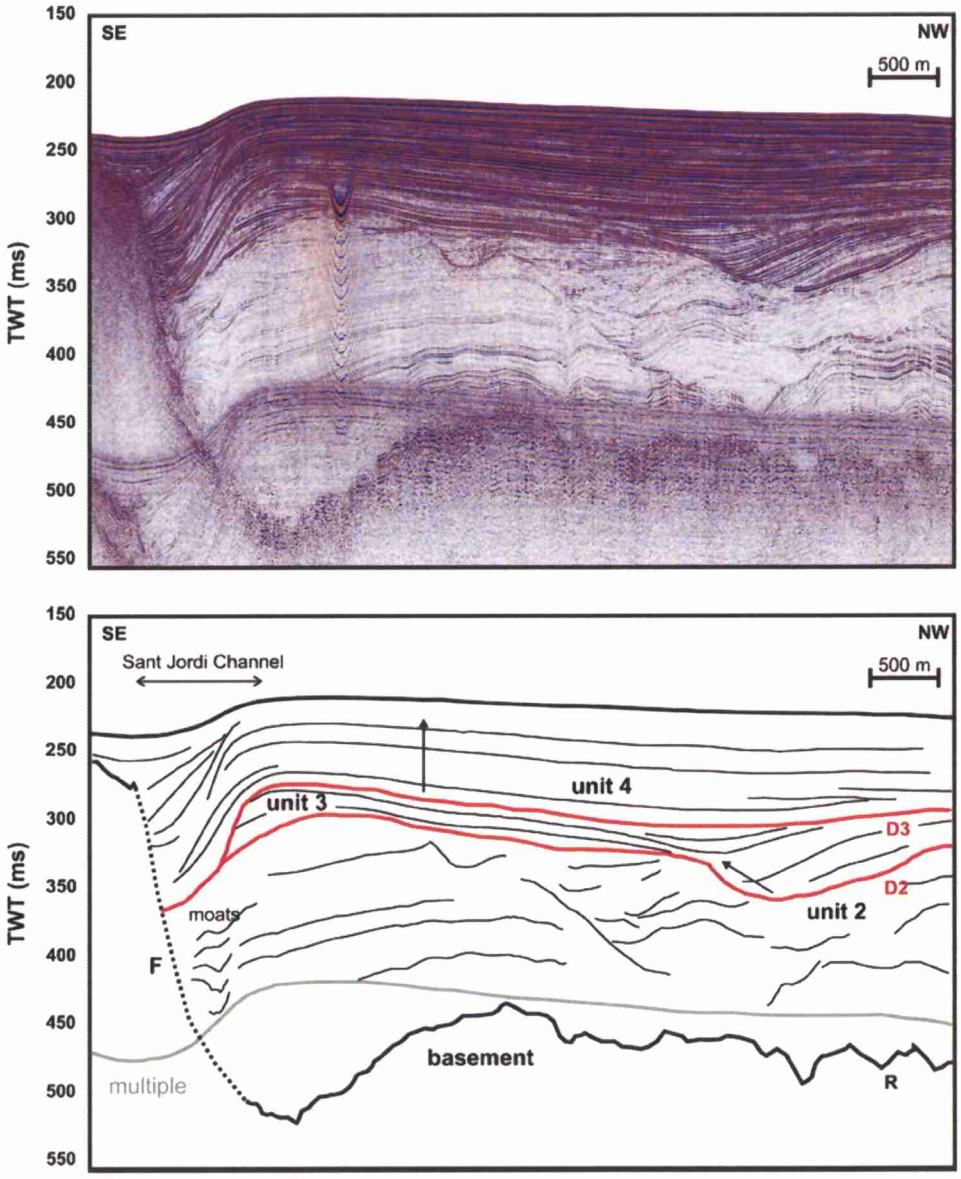

Fig. 5 Profile perpendicular to the basement fault, showing three (of the four) sedimentary units (for profile location, see Fig. 1b). Unit 1 is missing along this profile and the sedimentary sequence above the acoustic basement thus commences with unit 2. Close to the fault (*F*, *dashed line*), small moats are observed in this unit. Unit 3 displays parallel and prograding reflectors, filling a small channel in the north-western part of the profile. Unit 4 shows aggradation with evidence of reflectors dipping steeply towards the Sant Jordi Channel

Unit 4

The base of unit 4 (D3) increases in depth from the northeast (about 200 ms TWT below the sea surface) to the southwest (about 400 ms below the sea surface). Two distinct features are recognized: an amphitheatre-shaped depression in the west, up to 100 ms TWT deep, and a large channel along the basement fault, which is up to 60 ms deep and dips about 5° seawards (Figs. 5 and 6). The thickness of the unit varies between 10 and 110 ms TWT, the thickest deposits being found in the large channel (Fig. 5).

The reflectors of unit 4 show the highest amplitudes of the entire sedimentary series. In general, this unit displays parallel reflectors, onlapping onto a shallowing D3 in the northeast (Fig. 4). Here, ten subunits with reflector packages characterized by an alternation of high and low amplitudes are observed (Figs. 4, 5 and 6). The difference in amplitude between the reflector packages appears to be greater in unit 4 than in unit 3. Like unit 3, the subunits display a sigmoidal geometry along the basement fault, with progradation and downlap in the west and, in some parts, toplap above (Fig. 7). Most of these sigmoid-shaped subunits have a characteristic seismic facies expression, displaying a stronger outer reflector and an almost acoustically transparent core (Fig. 7).

In the northern part of the seismic grid are three channels, which display a prograding infill (Fig. 6). The largest channel, which cuts into D3, is filled by steeply dipping reflectors of unit 4 (Fig. 5). This infill is not recognized on all NW-SE-oriented profiles. In the eastern

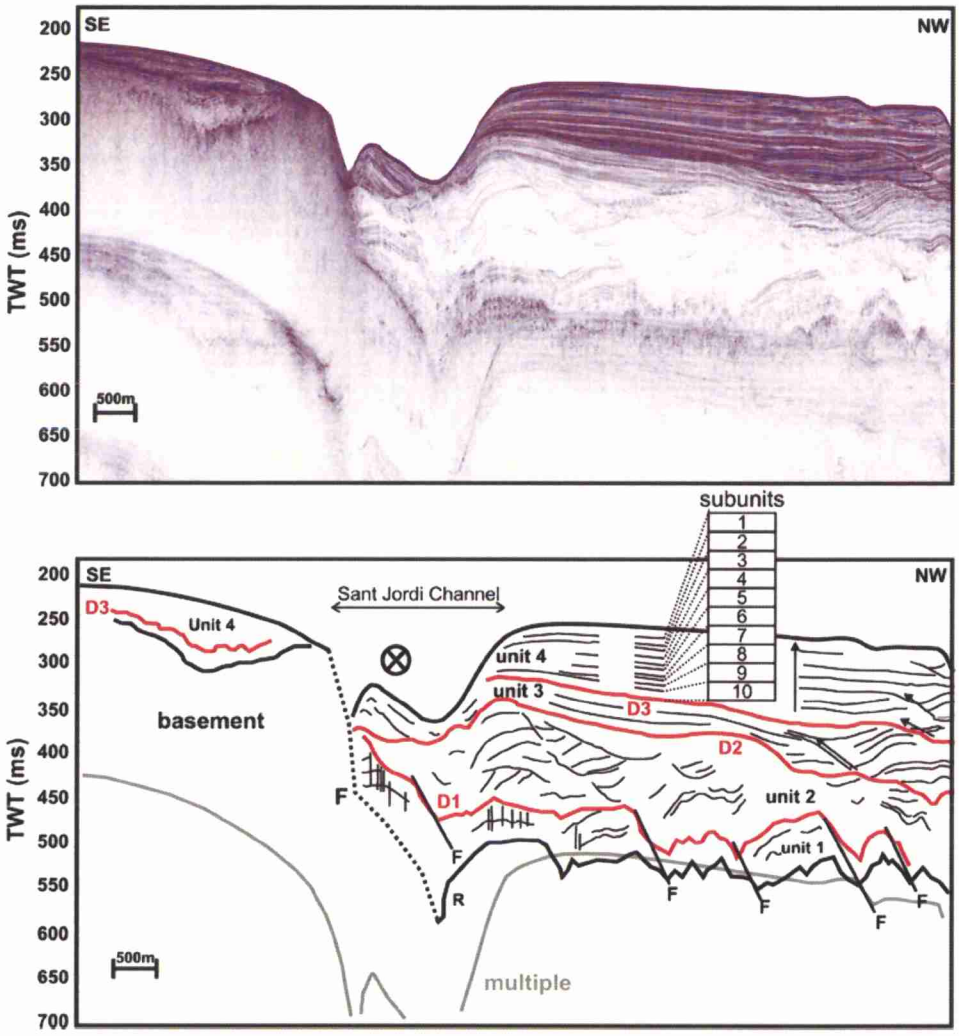

Fig. 6 Profile perpendicular to the basement fault (*F*, *dashed line*) showing the four units and three internal discontinuities (for profile location, see Fig. 1b). Unit 1 shows evidence of small vertical faults, as well as larger inclined faults. Unit 3 displays progradational infill of small cut-and-fill structures in the northwest and steeply dipping layers close to the basement fault in the southeast. Unit 4 is characterized by parallel, horizontally aggrading layers with a pronounced cyclicity of alternating high- and low-amplitude reflector packages. A selection of these cyclical subunits is indicated by the numbers *1* to *10*. The *encircled cross* denotes inferred current direction

part, the deposits are truncated by the Sant Jordi Channel (Figs. 3 and 6).

Discussion and conclusions

According to Pomar (1991), Hüssner et al. (2001) and Just et al. (2011), the observed basement in the vicinity of the study area is part of the Miocene Llucmajor reef platform and, more precisely, its open platform and slope facies. These facies consist of calcic siltstones, calcarenites and biostromes. Following post-Miocene flooding of the Mediterranean Sea and drowning of the reef complex, the Mallorca shelf and outer shelf became covered with a variably thick sedimentary succession.

Sedimentary processes

Based on the classifications of Faugères et al. (1999) and Rebesco et al. (2005), as well as accounting for existing knowledge on the oceanographic setting and regional bathymetry, the deposits along the south-western shelf of Mallorca can be interpreted as elongate-mounded, shallow-water contourite drifts. Their morphology is distinctly mounded and elongate in shape, whereas their internal configuration displays short discontinuous to chaotic reflectors, horizontal and low-inclination reflectors, and sigmoidal progradational reflectors. Moreover, there is a large variety of erosional features, including small cut-and-fill structures, larger drift-marginal moats and widespread discontinuities (Fig. 6). Erosional features are common to many contourite systems (Hernández-Molina et al. 2008), such as those observed in the Weddell Sea, Antarctica (Maldonado et al. 2005) and in the Gulf of Cadiz (García et al. 2009; Marchès et al. 2010). Chaotic and discontinuous reflectors associated with moats in the present study (Fig. 5) have been observed in similar deposits in the Le Danois drift in the Bay of Biscay (Van Rooij et al. 2010), and the Florida drift (Faugères et al. 1999). The complete system of drifts and erosional features on the Mallorca shelf is here

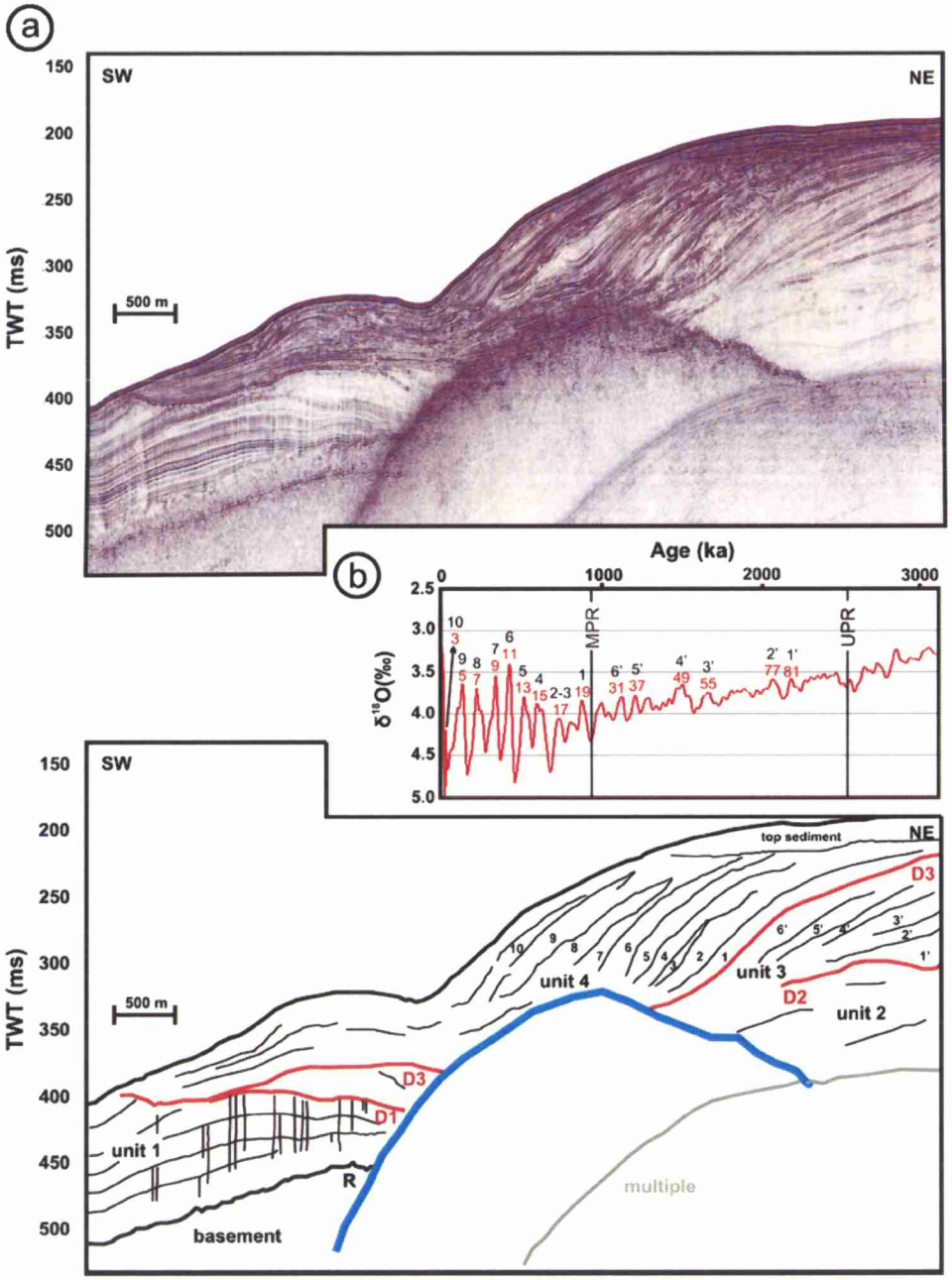

Fig. 7 **a** Profile along the Sant Jordi Channel parallel and immediately north of the basement fault (cf. Figs. 1 and 3). The interpreted profile is shown in the lower panel: *black lines* basement and sedimentary cover, *red lines* discontinuities, *blue line* note higher position of the basement to the south of the so-called basement fault. Unit 1 of the sedimentary cover is strongly faulted. The subunits of units 3 and 4 display sigmoidal shapes. **b** Correlation between subunits *(black numbers)* and marine isotopic stages (MISs, *red numbers*) for the profile (MIS curve extracted from Lisiecki and Raymo 2005; *MPR* mid-Pleistocene revolution, *UPR* upper Pliocene revolution)

referred to as the Mallorca shallow-water contourite depositional system (CDS).

In contrast to most deep-water contourite systems, the Mallorca CDS has not developed parallel to a margin but is aligned more or less perpendicular to it, generally parallel to the steep basement fault. It is here inferred that the current responsible for creating these deposits was deflected by the prominent fault-generated seafloor relief, being diverted towards the SW and aligning the contourite deposits in that direction. Indeed, the interaction of bottom currents with seafloor relief is known to be a common mechanism in the generation of contourite drifts (e.g. Cacchione et al. 1988; Faugères et al. 1999).

The onlapping infill on the south-eastern flank of the channels in units 3 and 4 (Figs. 5 and 6) suggests a sediment-loaded, bottom-hugging current flowing from the north and depositing sediments in the channels. This means that the present-day current pattern may have existed already during the deposition of these upper two units and may not have changed substantially since then. Inferring the current path or direction from the lower two units is more difficult because less current-related features are

observed. However, the presence of buried moats along the basement fault and small cut-and-fill structures in unit 2 suggests a very similar current pattern as proposed for the overlying two units. This implies that essentially the same current pattern may have persisted during the deposition of the entire sedimentary series.

Here, it is proposed that the Mallorca shallow-water CDS was deposited under the influence of a southward-flowing, bottom-hugging current. Within the present-day Mallorca Channel, there is an exchange between northward-flowing surface waters of Atlantic origin and southward-flowing, more saline waters derived from the Balearic Current (Pinot et al. 2002; Monserrat et al. 2008; Bardají et al. 2009). Hence, the southward-flowing offshoot of the Balearic Current is most probably responsible for shaping the contourite deposits because (1) the direction of the current agrees with the observed current-related features and (2) the Balearic Current is more saline, which makes it more likely to flow along the bottom of the Mallorca Channel, beneath the northward-moving Atlantic waters. Current velocities for this area are available only from modelling using the MIT (Massachusetts Institute of Technology) general circulation model (Marshall et al. 1997). The modelling results indicate bottom currents reaching 10 cm/s in this region (Hernández-Molina et al. 2011, this volume).

Within the Sant Jordi Channel, which traces the basement fault, there are marked basinward-dipping, progradational reflectors which show a sigmoidal geometry in the upper two units (Fig. 7). In general, these reflect a down-channel flow direction. It is proposed that the Sant Jordi Channel originated as a result of a stronger palaeo-Balearic Current deflected by the steep fault escarpment. Due to both the deflection and the steep seafloor relief, the current would have been intensified, leading to marked erosion and development of the contourite channel. A stronger current during the deposition of the upper two units is in accordance with the observation of higher-amplitude reflectors resulting from coarser-grained deposits. Episodic slope failure along the steep slopes (5°) of the Sant Jordi Channel is also evident in some of the sigmoidal subunits. The destabilization of sediment on steeper slopes has already been reported for the region by Acosta et al. (2002).

Stratigraphic evolution

Due to lack of local core and drilling data, no detailed chronostratigraphy can be established beyond that proposed by Stanley et al. (1976), who inferred the presence of Pliocene and Quaternary sedimentary series on top of a Miocene reef. This would imply that the shallow-water CDS is post-Miocene in age. Nevertheless, a tentative correlation is made here with the general stratigraphy proposed by Hernández-Molina et al. (2002) for Pliocene and Quaternary shelf sequences off the southern Iberian Peninsula, based on seismic profiles from the Alboran Sea and Gulf of Cadiz. In general, the shelf sequences have been subdivided into four major depositional units (1 to 4) separated by three major discontinuities: the lower Pliocene revolution (LPR, 4.2 Ma), the upper Pliocene revolution (UPR, 2.4 Ma) and the mid-Pleistocene revolution (MPR, 0.9 Ma). Note that the upper Pliocene revolution is now more correctly referred to as the base Quaternary discontinuity, since recalibration sets the base of the Quaternary at 2.58 Ma (Gibbard et al. 2010). Reference to the UPR is retained in the present study to avoid confusion with Hernández-Molina et al. (2002).

In the present dataset, a similar seismic stratigraphic framework can be discerned as that documented for the Alboran Sea and Gulf of Cadiz: four units subdivided by three major discontinuities. Furthermore, transparent seismic facies of Pliocene age, covered by deposits containing reflectors of higher amplitudes, have been observed throughout the Mediterranean and North Atlantic (Curzi et al. 1985; Alonso and Ercilla 2003). These arguments suggest that the two lower units (1 and 2), which contain reflectors of lower amplitudes (Figs. 4, 5 and 6), can be attributed a mainly Pliocene age, assuming that D2 correlates with the UPR and D1 with the LPR. Hence, the upper two units (3 and 4), which contain reflectors of higher amplitudes (Figs. 4, 5, 6 and 7), would be mainly Pleistocene in age, which in turn implies that D3 may be correlated to the MPR. The three discontinuities (D1, D2 and D3) bounding the four units may in each case indicate a major change in oceanographic conditions, involving changes in either sediment supply, sea level and/or current intensity. Similar observations have been made by Verdicchio and Trincardi (2008a) in shallow-water contourites from the Adriatic margin.

The probable erosional nature of discontinuity D1 cannot be determined solely by means of seismic data, notably because this surface is heavily faulted (Fig. 7). Discontinuity D1 is tentatively correlated with the LPR, being associated with a sea-level fall of about 50 m (Haq et al. 1987; Alonso and Maldonado 1992). Discontinuity D2 is clearly an erosional boundary (evidenced by the large incisions in unit 2) and can be associated with the UPR and a sea-level fall of about 50 m in the Late Pliocene. Since about 2.4 Ma, the onset of northern hemispheric glaciations and the establishment of the present-day oceanic circulation caused glacio-eustatic variations in sea level in the order of 50 m (Lowrie 1986; Haq et al. 1987). The erosional boundary D3 can be associated with the MPR, which has

been linked to a major change in climate: glacial cycles have shifted from 41-ka cycles (obliquity) to longer, eccentricity-controlled 100-ka cycles (Shackleton et al. 1990; Paillard 1998). This change in climatic trend is consistent with the high amplitudes of the reflectors and the large number of cyclical alternations observed in the upper unit (Figs. 6 and 7).

Compared to deep-water environments, continental shelves are more effectively and more repeatedly influenced by eustatic variations (Hernández-Molina et al. 2002; Verdicchio and Trincardi 2008b; Ridente et al. 2009). Shallow-water (or even subaerial) erosion and a large decrease in accommodation space can occur after sea-level falls. In turn, these factors can substantially influence bottom current regimes, in terms of both intensity and pathway. Indeed, Verdicchio and Trincardi (2008a) state that short-distance changes in the morphology of contourite systems may be caused by rapid changes in the current regime, controlled by climatic oscillations and shorter-term (seasonal) fluctuations in, for example, sediment availability or current strength.

The upper two units, plausibly of post-LPR age, display several features which can be attributed to climatic variations. Firstly, short-distance changes in morphology have been observed over a distance of only 10 km, including small channels, moats, continuous sub-horizontal parallel layers and steeply dipping layers (Fig. 6). Secondly, a cyclical pattern of subunits containing higher- and lower-amplitude reflector packages characterizes these upper two units (Figs. 4, 5 and 6). Thirdly, progradational sigmoidal subunits have been identified in a channel system along the basement fault (Fig. 7). Along the western Adriatic margin, such depositional changes have been linked to specific marine isotopic stages (MISs) and, thus, climatic variations (Ridente et al. 2009).

The subunits in units 3 and 4 are here tentatively correlated with interglacial periods and, hence, high sea-level stands (odd MISs; Fig. 7, MIS data extracted from Lisiecki and Raymo 2005). This may seem to not accommodate MIS 17, as it is characterized by two smaller sea-level rises separated by a minor fall. However, this may indeed be expressed in the sigmoidal subunits 2 and 3. Subunit 3 (which is thinner than the surrounding sigmoidal subunits) can be correlated to the youngest interglacial of this MIS (Fig. 7). The ten cyclical subunits outside the channel system can be correlated to MISs as well (Figs. 6 and 8). A similar approach can be attempted for the subunits of unit 3, although this is far more speculative than for the overlying unit. The sigmoidal subunits are less clearly expressed, the difference in amplitude between the subunits is smaller, a longer time span (2.4–0.9 Ma) is covered by a thinner unit (35 ms TWT, rather than 75 ms TWT for unit 4), and the variations in $\delta^{18}O$ values are smaller during this period. In this case, therefore, the six subunits have been correlated to the largest increases in $\delta^{18}O$ values (Fig. 7). A summary of the subunits of units 3 and 4, their associated MISs and their approximate ages is presented in Fig. 8.

In conclusion, the existence of a shallow-water contourite depositional system on the south-western Mallorca shelf sheds new light on factors controlling the localization and organization of shallow-water CDSs. These can be created by the interaction between surface currents and topographic features in conjunction with eustatic sea-level variations. To describe the CDS of the south-western Mallorca shelf in greater detail, an expansion of the existing seismic grid and the collection of cores would be required.

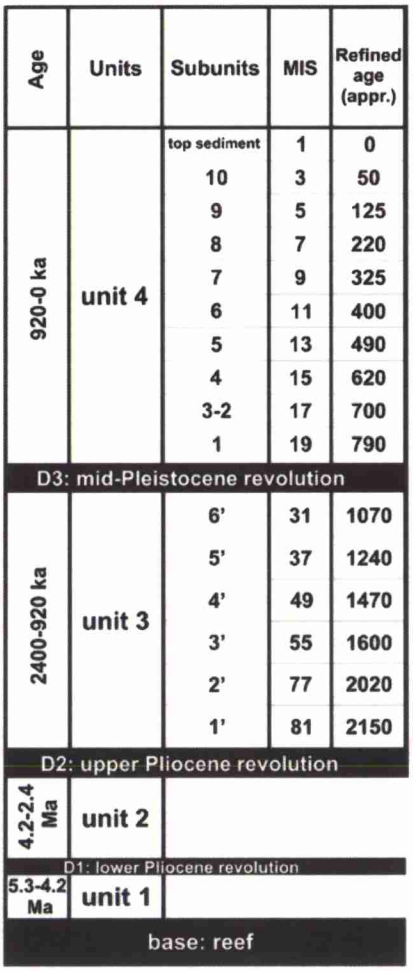

Fig. 8 Summary of sedimentary units, subunits and discontinuities on the shelf and shelf edge off south-western Mallorca, showing interpreted associations of the subunits with marine isotopic stages (MISs), together with their estimated ages (ka B.P.; latter data extracted from Hernández-Molina et al. 2002 and Lisiecki and Raymo 2005)

Acknowledgements The data for this paper have been acquired by the Vrije Universiteit Amsterdam, whom the authors wish to thank, especially Jeroen Kenter and Klaas Verwer for processing the data. The ISES (Integrated Solid Earth Science) program helped financing this project. Wim Versteeg and Koen De Rycker are acknowledged for the acquisition of the data. We would also like to acknowledge the technical "Kingdom" assistance from Lies De Mol and the corrections from Willem Vandoorne. Review comments from T. Nielsen and F. Trincardi improved the quality of the manuscript substantially.

References

Acosta J, Muñoz A, Herranz P, Palomo C, Ballesteros M, Vaquero M, Uchupi E (2001) Geodynamics of the Emile Baudot Escarpment and the Balearic Promontory, Western Mediterranean. Mar Petrol Geol 18:349–369. doi:10.1016/S0264-8172(01)00003-4

Acosta J, Canals M, López-Martínez J, Muñoz A, Herranz P, Urgeles R, Palomo C, Casamor JL (2002) The Balearic Promontory geomorphology (Western Mediterranean): morphostructure and active processes. Geomorphology 49:177–204. doi:10.1016/S0169-555X(02)00168-X

Acosta J, Canals M, Carbó A, Muñoz A, Urgeles R, Muñoz-Martín A, Uchupi E (2004) Sea floor morphology and Plio-Quaternary sedimentary cover of the Mallorca Channel, Balearic Islands, Western Mediterranean. Mar Geol 206:165–179. doi:10.1016/j.margeo.2004.02.008

Alonso B, Ercilla G (2003) Small turbidite systems in a complex tectonic setting (SW Mediterranean Sea): morphology and growth patterns. Mar Petrol Geol 19:1225–1240. doi:10.1016/S0264-8172(03)00036-9

Alonso B, Maldonado A (1992) Plio-Quaternary margin growth patterns in a complex tectonic setting: Northeastern Alboran Sea. Geo-Mar Lett 12(2/3):137–143. doi:10.1007/BF02084924

Bardají T, Goy JL, Zazo C, Hillaire-Marcel C, Dabrio CJ, Cabero A, Ghaleb B, Silva PG, Lario J (2009) Sea level and climate changes during OIS 5e in the Western Mediterranean. Geomorphology 104:22–37. doi:10.1016/j.geomorph.2008.05.027

Betzler C, Braga JC, Jaramillo-Vogel D, Römer M, Hübscher C, Schmiedl G, Lindhorst S (2011) Late Pleistocene and Holocene cool-water carbonates of the Western Mediterranean Sea. Sedimentology 58:643–669. doi:10.1111/j.1365-3091.2010.01177.x

Cacchione D, Schwab W, Noble M, Tate G (1988) Internal tides and sediment movement on Horizon Guyot, Mid-Pacific Mountains. Geo-Mar Lett 8(1):11–17. doi:10.1007/BF02238001

Curzi PV, Fornos J, Mauffret A, Sartori R, Serra J, Zitellini E, Borsetti AM, Canals M, Castellarin A, Pomar L, Rossi PL, Sabat F (1985) The South-Balearic Margin (Menorca Rise): objectives and preliminary results of the cruise Bal-84. Rend Soc Geol Ital suppl 8:91–96

Ercilla G, Baraza J, Alonso B, Estrada F, Casas D, Farran M (2002) The Ceuta Drift, Alboran Sea, southwestern Mediterranean. In: Stow D, Pudsey C, Howe J, Faugères J, Viana A (eds) Deep-water contourite systems: modern drifts and ancient series, seismic and sedimentary characteristics. Geol Soc Lond Mem 22:155–170

Faugères J, Stow DAV (1993) Bottom-current-controlled sedimentation: a synthesis of the contourite problem. Sed Geol 82:287–297. doi:10.1016/0037-0738(93)90127-Q

Faugères J-C, Stow DAV, Imbert P, Viana A (1999) Seismic features diagnostic of contourite drifts. Mar Geol 162:1–38. doi:10.1016/S0025-3227(99)00068-7

Frigola J, Moreno A, Cacho I, Canals M, Sierro FJ, Flores JA, Grimalt JO (2008) Evidence of abrupt changes in Western Mediterranean Deep Water circulation during the last 50 kyr: a high-resolution marine record from the Balearic Sea. Quat Int 181:88–104. doi:10.1016/j.quaint.2007.06.016

García M, Hernández-Molina FJ, Llave E, Stow DAV, León R, Fernández-Puga MC, Díaz del Río V, Somoza L (2009) Contourite erosive features caused by the Mediterranean Outflow Water in the Gulf of Cadiz: quaternary tectonic and oceanographic implications. Mar Geol 257:24–40. doi:10.1016/j.margeo.2008.10.009

Gibbard PL, Head MJ, Walker MJC (2010) Formal ratification of the Quaternary System/Period and the Pleistocene Series/Epoch with a base at 2.58 Ma. J Quat Sci 25:96–102. doi:10.1002/jqs.1338

Haq BU, Hardenbol J, Vail PR (1987) Chronology of fluctuating sea levels since the Triassic. Science 235:1156–1167. doi:10.1126/science.235.4793.1156

Heezen BC, Hollister CD, Ruddiman WF (1966) Shaping of the continental rise by deep geostrophic currents. Science 152:502–508. doi:10.1126/science.152.3721.502

Hernández-Molina FJ, Somoza L, Vazquez JT, Lobo F, Fernández-Puga MC, Llave E, Díaz-del Río V (2002) Quaternary stratigraphic stacking patterns on the continental shelves of the southern Iberian Peninsula: their relationship with global climate and palaeoceanographic changes. Quat Int 92:5–23. doi:10.1016/S1040-6182(01)00111-2

Hernández-Molina FJ, Llave E, Stow DAV (2008) Continental slope contourites. In: Rebesco M, Camerlenghi A (eds) Contourites. Developments in sedimentology, vol 60. Elsevier, Amsterdam, pp 379–407

Hernández-Molina FJ, Serra N, Stow DAV, Llave E, Ercilla G, Van Rooij D (2011) Along-slope oceanographic processes and sedimentary products around the Iberian margin. Geo-Mar Lett (in press). doi:10.1007/s00367-011-0242-2

Hüssner H, Roessler J, Betzler C, Petschick R, Peinl M (2001) Testing 3D computer simulation of carbonate platform growth with REPRO: the Miocene Llucmajor carbonate platform (Mallorca). Palaeogeogr Palaeoclimatol Palaeoecol 175:239–247. doi:10.1016/S0031-0182(01)00374-1

Just J, Hübscher C, Betzler C, Lüdmann T, Reicherter K (2011) Erosion of continental margins in the Western Mediterranean due to sea-level stagnancy during the Messinian Salinity Crisis. Geo-Mar Lett 31(1):51–64. doi:10.1007/s00367-010-0213-z

Lisiecki LE, Raymo ME (2005) A Plio-Pleistocene stack of 57 globally distributed benthic $\delta^{18}O$ records. Paleoceanography 20: PA1003. doi:10.1029/2004PA001071

Lowrie A (1986) Model for fine-scale movements associated with climate and sea level changes along the Louisiana shelfbreak growth faults. Gulf Coast Assoc Geol Soc Trans 36:497–508. doi:10.1306/A1ADDCB3-0DFE-11D7-8641000102C1865D

Maldonado A, Barnolas A, Bohoyo F, Escutia C, Galindo-Zaldívar J, Hernández-Molina J, Jabaloy A, Lobo FJ, Nelson CH, Rodríguez-Fernández J, Somoza L, Vázquez J-T (2005) Miocene to Recent contourite drifts development in the Northern Weddell Sea (Antarctica). Global Planet Change 45:99–129. doi:10.1016/j.gloplacha.2004.09.013

Marchès E, Mulder T, Gonthier E, Cremer M, Hanquiez V, Garlan T, Lecroart P (2010) Perched lobe formation in the Gulf of Cadiz: interactions between gravity processes and contour currents (Algarve Margin, Southern Portugal). Sed Geol 229:81–94. doi:10.1016/j.sedgeo.2009.03.008

Marshall J, Adcroft A, Hill C, Perelman L, Heisey C (1997) A finite-volume, incompressible Navier Stokes model for studies of the ocean on parallel computers. J Geophys Res 102:5753–5766. doi:10.1029/96jc02775

Monserrat S, López-Jurado JL, Marcos M (2008) A mesoscale index to describe the regional circulation around the Balearic Islands. J Mar Systems 71:413–420. doi:10.1016/j.jmarsys.2006.11.012

Paillard D (1998) The timing of Pleistocene glaciations from a simple multiple-state climate model. Nature 391:378–381. doi:10.1038/34891

Pickard GL, Emery WJ (1990) Descriptive physical oceanography: an introduction, 5th edn. Pergamon Press, Oxford

Pinot JM, López-Jurado JL, Riera M (2002) The CANALES experiment (1996–1998). Interannual, seasonal, and mesoscale variability of the circulation in the Balearic Channels. Prog Oceanogr 55:335–370. doi:10.1016/S0079-6611(02)00139-8

Pomar L (1991) Reef geometries, erosion surfaces and high-frequency sea-level changes, upper Miocene Reef Complex, Mallorca, Spain. Sedimentology 38:243–269. doi:10.1111/j.1365-3091.1991.tb01259.x

Rebesco M, Richard CS, Cocks LRM, Ian RP (2005) Sedimentary environments: contourites. In: Encyclopedia of Geology. Elsevier, Oxford, pp 513–528

Ridente D, Trincardi F, Piva A, Asioli A (2009) The combined effect of sea level and supply during Milankovitch cyclicity: evidence from shallow-marine $\delta^{18}O$ records and sequence architecture (Adriatic margin). Geology 37:1003–1006. doi:10.1130/g25730a.1

Shackleton NJ, Berger A, Peltier WR (1990) An alternative astronomical calibration of the lower Pleistocene timescale based on ODP Site 677. Trans R Soc Edinburgh Earth Sci 81:251–261

Stanley DJ, Got H, Kenyon NH, Monaco A, Weiler Y (1976) Catalonian, Eastern Betic, and Balearic margins: structural types and geologically recent foundering of the Western Mediterranean Basin. Smithsonian Contributions to the Earth Sciences 20

Stow DAV, Ogawa Y, Lee IT, Mitsuzawa K (2002) Neogene contourites, Miura-Boso forearc basin, SE Japan. In: Stow DAV, Pudsey C, Howe J, Faugères J, Viana A (eds) Deep-water contourite systems: modern drifts and ancient series, seismic and sedimentary characteristics. Geol Soc Lond Mem 22:409–419

Van Rooij D, Iglesias J, Hernández-Molina FJ, Ercilla G, Gomez-Ballesteros M, Casas D, Llave E, De Hauwere A, Garcia-Gil S, Acosta J, Henriet JP (2010) The Le Danois Contourite Depositional System: interactions between the Mediterranean Outflow Water and the upper Cantabrian slope (North Iberian margin). Mar Geol 274:1–20. doi:10.1016/j.margeo.2010.03.001

Verdicchio G, Trincardi F (2008a) Mediterranean shelf-edge muddy contourites: examples from the Gela and South Adriatic basins. Geo-Mar Lett 28(3):137–151. doi:10.1007/s00367-007-0096-9

Verdicchio G, Trincardi F (2008b) Shallow-water contourites. In: Rebesco M, Camerlenghi A (eds) Contourites. Developments in sedimentology, vol 60. Elsevier, Amsterdam, pp 409–433

Viana AR, Faugères JC, Stow DAV (1998) Bottom-current-controlled sand deposits—a review of modern shallow- to deep-water environments. Sed Geol 115:53–80. doi:10.1016/S0037-0738(97)00087-0

Viana AR, Almeida W Jr, Nunes MCV, Bulhoes EM (2007) The economic importance of contourites. Geol Soc Lond Spec Publ 276:1–23. doi:10.1144/gsl.sp.2007.276.01.01

Werner FE, Viúdez A, Tintoré J (1993) An exploratory numerical study of the currents off the Southern coast of Mallorca including the Cabrera Island complex. J Mar Systems 4:45–66. doi:10.1016/0924-7963(93)90019-I